FFI RAPPORT

MID-INFRARED OPTICAL PARAMETRIC OSCILLATORS BASED ON PERIODICALLY-POLED LITHIUM NIOBATE

ARISHOLM Gunnar, STENERSEN Knut, RUSTAD Gunnar,
LIPPERT Espen, HAAKESTAD Magnus

FFI/RAPPORT-2002/02830

FFIE/792/115

Approved
Kjeller 25 juni 2002

Stian Løvold
Director of Research

MID-INFRARED OPTICAL PARAMETRIC OSCILLATORS BASED ON PERIODICALLY-POLED LITHIUM NIOBATE

ARISHOLM Gunnar, STENERSEN Knut, RUSTAD Gunnar, LIPPERT Espen, HAAKESTAD Magnus

FFI/RAPPORT-2002/02830

FORSVARETS FORSKNINGSINSTITUTT
Norwegian Defence Research Establishment
P O Box 25, NO-2027 Kjeller, Norway

FORSVARETS FORSKNINGSINSTITUTT (FFI)
Norwegian Defence Research Establishment

P O BOX 25
N0-2027 KJELLER, NORWAY

UNCLASSIFIED

SECURITY CLASSIFICATION OF THIS PAGE
(when data entered)

REPORT DOCUMENTATION PAGE

1) PUBL/REPORT NUMBER	2) SECURITY CLASSIFICATION	3) NUMBER OF PAGES
FFI/RAPPORT-2002/02830	UNCLASSIFIED	31
1a) PROJECT REFERENCE	**2a) DECLASSIFICATION/DOWNGRADING SCHEDULE**	
FFIE/792/115	-	

4) TITLE

MID-INFRARED OPTICAL PARAMETRIC OSCILLATORS BASED ON PERIODICALLY-POLED LITHIUM NIOBATE

5) NAMES OF AUTHOR(S) IN FULL (surname first)

ARISHOLM Gunnar, STENERSEN Knut, RUSTAD Gunnar, LIPPERT Espen, HAAKESTAD Magnus

6) DISTRIBUTION STATEMENT

Approved for public release. Distribution unlimited. (Offentlig tilgjengelig)

7) INDEXING TERMS

IN ENGLISH:	IN NORWEGIAN:
a) Optical parametric oscillators	a) Optiske parametriske oscillatorer
b) Nonlinear optics	b) Ikke-lineær optikk
c) Infrared sources	c) Infrarøde kilder
d) Optical materials	d) Optiske materialer
e)	e) Infrarøde stråler - Motmidler

THESAURUS REFERENCE:

8) ABSTRACT

A study has been conducted of mid-infrared optical parametric oscillators (OPOs) based on periodically poled lithium niobate (PPLN) as the nonlinear optical material. Experiments have been performed with a number of 1.06 μm pump sources and OPO resonator configurations, in both pulsed and cw mode of operation. The OPO idler wavelength could be tuned across the 3.1-3.8 μm region, by using 8 different PPLN grating periods on the same crystal. In nearly all cases, the measured pump-to-idler conversion efficiency was in the range of 7-9 %, and the idler output power was in the range of 1-1.4 W. A notable exception was the result obtained with a monolithic OPO resonator with very low signal and idler feedback, and a short pump pulse (<10 ns). In this case, an output power of almost 1 W was obtained at only 5.3 W pump power, corresponding to 18 % conversion efficiency. This was the maximum pump power that could be used without risking optical damage. The reason for the high efficiency in this case is probably reduced back-conversion due to the low signal and idler feedback. Using the totally available 18 W pump power to pump 3 different PPLN OPOs, there is potential for achieving 3 W of mid-infrared output at 3 different mid-infrared wavelengths with this configuration. The conversion efficiency obtained in cw operation was 8-9 %, which is more than a factor of 2 below the best results reported in the literature. It is suspected that the conversion efficiency was limited by thermal lens effects caused by a small residual absorption at the pump and signal wavelengths in the crystals used in the cw experiments.

9) DATE	AUTHORIZED BY	POSITION
	This page only	
25 juni 2002	Stian Løvold	Director of Research

ISBN-82-464-624-8

UNCLASSIFIED

SECURITY CLASSIFICATION OF THIS PAGE
(when data entered)

CONTENTS

MID-INFRARED OPTICAL PARAMETRIC OSCILLATORS BASED ON PERIODICALLY-POLED LITHIUM NIOBATE

1 INTRODUCTION

There is currently an urgent military need for efficient tunable laser sources in the 3-5 μm (mid-IR) spectral band. Such sources are key components in directive infrared countermeasure (DIRCM) systems against military infrared sensors, such as missile seekers and thermal imagers. Such countermeasure acts may include either deception, dazzling, or destruction of the infrared sensor. FFI has taken interest in this subject, both in order to investigate the vulnerability of Norwegian military sensors to such countermeasures, and in order to evaluate the possibility of employing such countermeasures against enemy sensors, such as IR missile seekers.

Practical use of such countermeasures requires access to efficient laser sources, which should preferably be tunable to any wavelength within the 3-5 μm spectral band. In the past there has been a lack of such sources. However, the advent of efficient diode pumped solid-state lasers, combined with efficient nonlinear wavelength shifters, has recently paved the way for development of practical tunable mid-IR countermeasure sources, and the first of such systems are about to be installed on air platforms for protection against IR homing missiles [1, 2].

FFI has an activity devoted to development of such sources for experimental studies of countermeasure effects. This activity involves development of diode pumped solid state lasers in the 1-2 μm region (near-IR) as the primary laser sources, as well as nonlinear wavelength shifters in order to access the 3-5 μm band. The wavelength shifters are various types of so-called optical parametric oscillators (OPOs), which consist of one or more nonlinear optical crystals placed inside an optical resonator. The OPO is pumped by the output from the near-IR primary laser source and generates two new electromagnetic waves at longer infrared wavelengths. Energy conservation requires that the sum of the frequencies of the generated waves is equal to the pump frequency. The generated frequencies (or wavelengths) can in many cases be tuned across wide spectral regions by altering the so-called phase-matching condition of the nonlinear process. This is most commonly achieved by rotating the nonlinear crystal or by altering its temperature. This ability to generate tunable laser radiation makes OPOs ideal countermeasure sources, since the wavelength cannot easily be predicted by the counterpart, making protective measures against it more difficult.

The purpose of this report is to present results obtained at FFI with one of the most promising nonlinear materials, so-called periodically-poled lithium niobate (PPLN), which is used to generate radiation in the 3-4 μm region. Results obtained with a number of OPO configurations, in both pulsed and continuous-wave mode of operation, will be presented.

Section 2 of the report gives a brief overview of the main options for combining pump sources and OPOs in order to obtain efficient generation of mid-IR laser radiation. The nonlinear conversion process in the PPLN material used in this work, is phase-matched by a special technique, commonly referred to as quasi-phase-matching. This is explained in Section 3, which also discusses other material properties of PPLN. The experimental configurations and results are discussed in Section 4, and conclusions are given in Section 5.

2 PRINCIPAL MID-IR OPO OPTIONS

There are a number of options for combining primary laser sources and wavelength shifters in order to reach the mid-IR wavelength bands, which include the 3-5 µm and 8-12 µm regions. The main options studied at FFI are sketched in Figure 2.1. The nonlinear wavelength shifters, indicated by boxes with broken lines in the figure, are optical parametric oscillators (OPOs) based on different nonlinear materials (PPLN, KTP, and ZGP). PPLN (periodically poled lithium niobate) is transparent from below 1 µm to about 4 µm wavelength and can be used to shift the output from a Nd:YAG laser to the 3-4 µm band in a single OPO stage (option (a)). In order to cover the entire 3-5 µm band or the 8-12 µm band it is necessary to employ a nonlinear material which is transparent across these bands. The only available practical material for this purpose is ZGP (zinc germanium phosphide), with a transparency range from about 2 µm to 10 µm, which precludes direct pumping with Nd:YAG. This means that there is a need for a pump source at approximately 2 µm wavelength or higher. The principal options for achieving this is either to include an intermediate OPO stage based on e g KTP (potassium titanyl phosphate) in order to reach 2 µm (option (b)), or to develop a 2 µm laser source based on Tm and Ho, as in option (c).

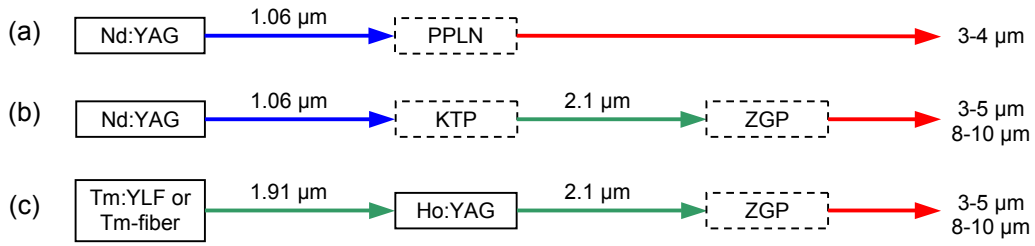

Figure 2.1 Principal options for nonlinear wavelength conversion to the 3-5 µm and 8-12 µm bands. The boxes with solid lines are lasers, and the boxes with broken lines are optical parametric oscillators.

We are developing both the pump lasers [3, 4] and the OPOs [5-10] for these schemes. This report discusses experiments performed at FFI with option (a), using a number of different OPO configurations and pump sources.

3 QUASI PHASE MATCHING BY PERIODIC POLING IN PPLN

3.1 Quasi phase-matching

For the nonlinear conversion to be efficient it is required that the relative phase of the interacting beams remains constant as they propagate through the nonlinear medium [11]. This is generally referred to as the *phase-matching requirement*. Due to dispersion (the refractive index of the medium changes with frequency), this requirement cannot generally be satisfied in isotropic media. Therefore, nonlinear conversion devices are normally based on anisotropic materials, where phase-matching can be achieved by choosing different polarizations for the interacting waves; so-called birefringent phase-matching. This method of phase-matching not only restricts the number of available nonlinear materials. It also restricts the allowed propagation directions and polarizations in such a way that the resulting effective nonlinear susceptibility is generally far below the maximum value for a given material. In addition, unless phase-matching can be achieved for propagation along one of the crystal axes (so-called noncritical phase-matching), there will also be a spatial walk-off between the beams, which limits the interaction distances and tends to distort the beam profiles. Finally, even for birefringent materials, it is not always possible to achieve phase matching for a given set of pump and signal frequencies, even if these frequencies are all within the crystal's transparency range.

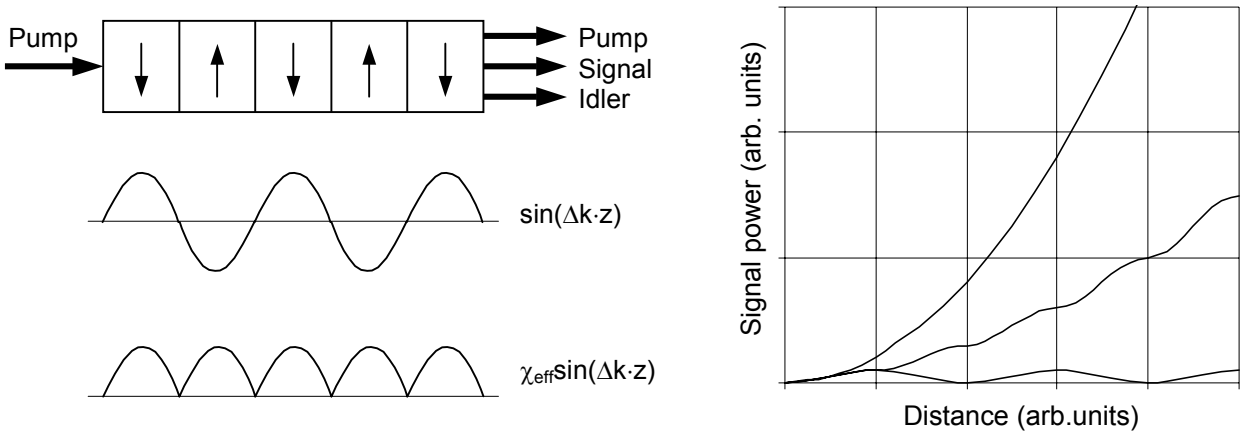

Figure 3.1: Principle of quasi phase-matching (QPM).
Left: QPM-material where the crystal orientation is inverted for every half-period of the driving term sin(Δk·z) in the coupled wave equation, where Δk is the bulk phase mismatch. The effective driving term χ_{eff} sin(Δk·z) is thereby rectified. Right: Signal growth through the material (middle curve – with QPM, lower curve – bulk material with phase mismatch Δk, upper curve – bulk material with Δk=0).

A solution to these problems is to employ so-called quasi-phase-matching (QPM), as illustrated in Figure 3.1. In QPM-devices it is common to choose a beam propagation direction in the crystal, as well as polarizations, which lead to maximum nonlinear susceptibility and

zero walk-off. In a normal nonlinear material, this would mean that the phase-matching condition could not be satisfied, and the energy would be transferred periodically forth and back between the pump and the signals through the crystal, with a resulting negligible energy conversion. The trick played in QPM-devices is to invert the crystal orientation for every half-period of these oscillations. This is equivalent to changing the sign of the nonlinear susceptibility for every half-period, or, equivalently, to change the phase in the driving term in the coupled wave equations by π. The net effect is that the energy transfer oscillations are rectified, such that energy is always transferred from the pump to the signals in all half-periods [12].

3.2 Methods of quasi phase matching

One method of achieving QPM is to use a stack of thin plates of the bulk material, where the crystal orientation is reversed from plate to plate. This has been done with GaAs, where a large number of plates have been bonded together by diffusion bonding [13]. The problem has been that the QPM-period is typically very short (tens of μm), so that a large number of plates are needed in order to obtain a sufficient interaction length and sufficient gain. The optical loss through all the bonded interfaces thereby becomes a major limitation. Recently, another technique has been invented, where a QPM crystal can be grown directly on a substrate on which the crystal orientation has been altered periodically by a special patterning technique [14]. This technique holds promise for efficient production of QPM crystals, but substantial development work is still required before this can become a practical method. The most successful method of producing QPM crystals has been applied to ferroelectric materials. In such materials the periodic inversion of the crystal orientation is achieved by periodically reversing the polarity of the ferroelectric crystal domains. This can be achieved by applying a high-voltage pulse across a bulk crystal, on which a lithographically defined periodic electrode pattern has been deposited. This method was first successfully applied to lithium niobate ($LiNbO_3$), and such QPM material is commonly denoted periodically poled lithium niobate (PPLN) [15-17]. The periodic poling technique has later also been applied to other materials, such as KTP (PPKTP) and RTA (PPRTA) [18, 19].

3.3 Properties of periodically poled lithium niobate (PPLN)

PPLN is transparent for wavelengths up to about 4 μm, as shown in Figure 3.2. For idler wavelengths above approximately 3.7 μm the increasing absorption leads to increased optical loss and, for high average powers, also to heating, thermal lensing, and thermally induced phase mismatch. With the PPLN crystals used in our experimental work, the maximum available idler wavelength was about 3.8 μm, so there was relatively little heating caused by absorption of the idler. In fact, a small residual absorption at the pump and signal wavelengths probably contributed more than the idler to heating of the crystal.

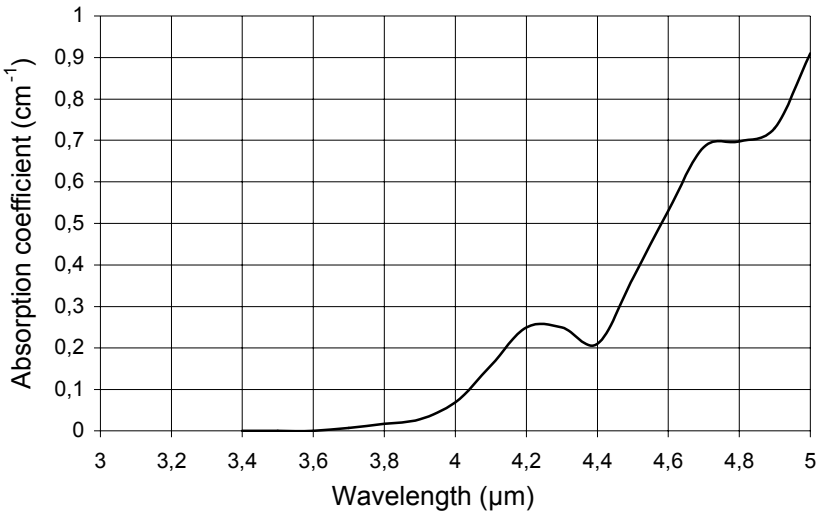

Figur 3.2: Absorption spectrum for PPLN [17]

The main advantages of PPLN over standard bulk $LiNbO_3$ are the lack of spatial walk-off and the high optical nonlinearity, which stems from the optimal choice of propagation direction and polarization. The effective nonlinear coefficient is about 17 pm/V [17]. The high gain implies that high conversion efficiency can be obtained for quite modest pump intensities, which means that problems with optical damage can be reduced. In fact, the gain is so high that efficient operation can be obtained even for cw-pumped singly resonant OPOs [17, 20]. One problem with $LiNbO_3$ in general is the susceptibility of the material to photorefractive effects, which tend to destroy the optical quality of the crystal when it is pumped by high intensity 1.06 µm radiation. The problem is caused by the presence of a small amount of (non-phase-matched) frequency-doubled pump light (at 532 nm), which is absorbed by impurities in the crystal. The common method of suppressing the photorefractive damage is to heat the crystal during OPO operation. The required operation temperature for PPLN is typically in the range of 150-200 °C, and is generally highest for cw-operation [17]. The alternating ferroelectric domain polarity, as well as the high nonlinearity, give PPLN an advantage over bulk $LiNbO_3$ with respect to photorefractive effects [17].

PPLN is available from commercial sources in 0.5 mm and 1 mm thickness and crystal lengths up to 50 mm. The longest crystals are used for cw-pumping, where the gain is much smaller than with Q-switched pulse pumping. Commercial vendors typically offer crystals with a number of different grating periods on the same crystal, each grating being approximately 1 mm wide. The different grating periods yield different signal and idler wavelengths for a given pump wavelength and crystal temperature.

We have studied experimentally a number of PPLN OPO configurations under both pulsed and cw operation, using Nd-lasers at 1.06 µm wavelength as pump sources. The configurations and experimental results are discussed in Section 4.

4 PPLN OPO EXPERIMENTS

4.1 PPLN crystals

The PPLN crystals used in the experimental work reported here were purchased from Crystal Technology, Inc (US). The crystals had 8 gratings with periods ranging from 28.5 μm to 29.9 μm. When pumped at 1.06 μm, the OPO idler wavelength ranged from approximately 3.8 μm (for 28.5 μm period) to 3.1 μm (for 29.9 μm period), at a typical crystal temperature of 190 °C. The idler wavelength decreases with temperature by 2-3 nm/K.

4.2 OPO resonator options

There are a number of possible options for the OPO resonator configuration. For example, there is a choice between singly- or doubly-resonant operation, i.e. whether to oscillate only the signal wavelength or both the signal and the idler. The latter gives a lower pump threshold but also generally leads to significant output power fluctuations. The fluctuations can be avoided or reduced if techniques for active stabilization of the resonator length are implemented in order to achieve simultaneous resonance of both the signal and the idler waves (in this case both waves should more correctly be called signal waves). This has not been implemented in our experiments, since the gain is generally sufficient to operate well above threshold in singly-resonant mode. In this case all of the idler should be coupled out through an AR-coated output mirror.

A second choice concerns whether to use a linear (standing wave) resonator or a ring resonator. A linear resonator with two mirrors is generally simpler and easier to align than a ring resonator. In such a resonator one may also choose to double-pass the pump beam through the PPLN crystal in order to increase the OPO gain, by reflecting the pump at the output mirror. This has the disadvantage that a Faraday isolator may have to be inserted between the pump laser and the OPO in order to avoid feedback into the pump laser. Such isolation may even be required with a nominally single-pass-pumped linear resonator, since there will always be some feedback due to imperfect mirror AR coatings. In this respect, a ring resonator offers some important advantages over the linear resonator. Another important feature of the ring configuration is that negligible feedback of the idler can be obtained, ensuring almost perfect singly resonant operation. This helps to minimize power fluctuations and suppresses back-conversion from signal and idler to the pump when the OPO is operated far above threshold. Moreover, for a given crystal length, a ring resonator provides a smaller round-trip time, and thereby a smaller signal build-up time, than a standing-wave resonator, and it provides a smaller total intracavity fluence. Finally, for OPOs operated at high average power, the use of a ring resonator reduces thermal lensing effects on the signal, since the signal passes through the crystals only once per roundtrip.

In our experiments we have chosen to employ only single-pass pumping also in the case of a linear resonator in order to prevent feedback to the pump laser. As will be seen in the case of pulsed OPO operation, there was not any significant difference in conversion efficiency for the

linear and ring resonators in our experiments, so the main advantage of the ring resonator was the relaxed need for optical isolation between the pump and the OPO.

4.3 Pulsed operation

4.3.1 Linear resonator

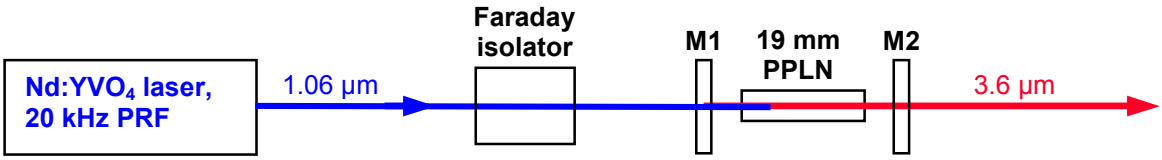

Figure 4.1 Linear OPO setup

In the first configuration the OPO resonator was linear with a 19 mm long and 1 mm thick PPLN crystal, as shown in Figure 4.1. A Faraday isolator was used in order to prevent feedback to the pump laser.

The pump source was a commercial Nd:YVO_4 laser (Spectra Physics, Model T80-YHP40-106Q) with excellent beam quality ($M^2 \approx 1.2$). It could be operated in Q-switched mode over a wide range of pulse rates, 1-100 kHz, as well as in cw-mode (see Section 4.4). The average available pump power increased with increasing pulse rate, but the increase was fairly small for pulse rates above 20 kHz (≈ 15 W at 20 kHz and 18 W at 100 kHz). The pulse length also increased with increasing pulse rate (≈ 30 ns at 10 kHz, 35 ns at 20 kHz, 45 ns at 40 kHz, 70 ns at 80 kHz). A primary goal in these experiments was to maximize the OPO output power, which is the product of the pump power and the conversion efficiency. Since the pump power increased with increasing pulse rate, it was therefore natural to use a pulse rate of at least 20 kHz. The OPO gain and conversion efficiency depend on a number of parameters, i.e. the pump pulse energy, pump spot size, pump pulse length, crystal length, OPO output coupling, resonator losses, etc. In general, a high conversion efficiency is most easily obtained for high pump pulse energies, and we therefore decided to optimize the OPO a pulse rate of 20 kHz. The pump was focused to a slightly asymmetric spot with a diameter in the two orthogonal directions of 490 µm x 420 µm ($FW1/e^2M$).

The OPO resonator was approximately 25 mm long, with flat mirrors. The mirror reflectivities at the pump, signal, and idler waves were 15 %, ≈ 100 %, and 13 %, respectively, for the input mirror (M1) and 20 %, 55 %, and 5 % for the output coupler (M2). The reflectivity of the PPLN end faces was 2-3 % for the pump and less than 1 % for the signal and idler. Experiments were performed with a PPLN grating period of 29.1 µm and a PPLN temperature of 160 °C, which resulted in an idler wavelength of about 3.6 µm. Under these conditions we obtained the results shown in Figure 4.2. The conversion efficiency from pump to idler at the maximum pump is about 7.5 %, and the slope efficiency is 11-12 %.

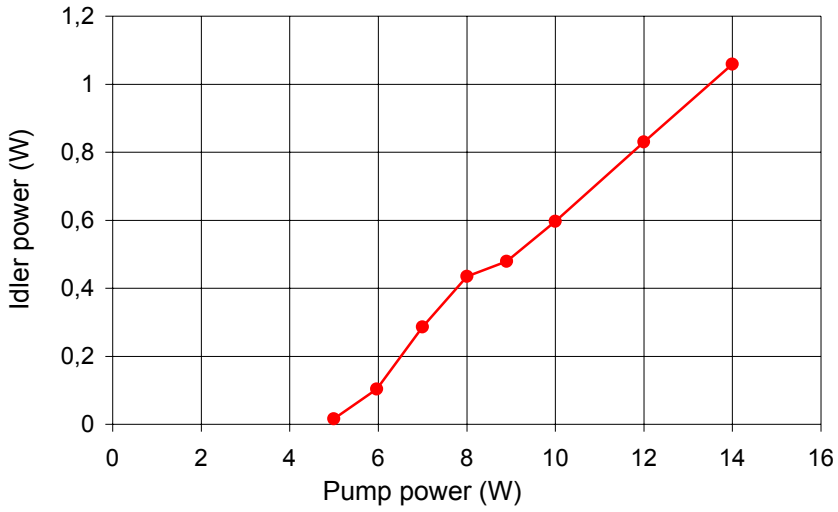

Figure 4.2: 3.6 µm idler output power vs pump power. The pump power is the total power incident on the OPO input mirror. The idler output power is corrected for a 6 % loss in a filter, which was used to block the residual pump and the signal at the output.

The beam profile was fairly smooth and Gaussian-like as shown in Figure 4.3, but the beam quality (M^2 – factor) was not measured in these experiments.

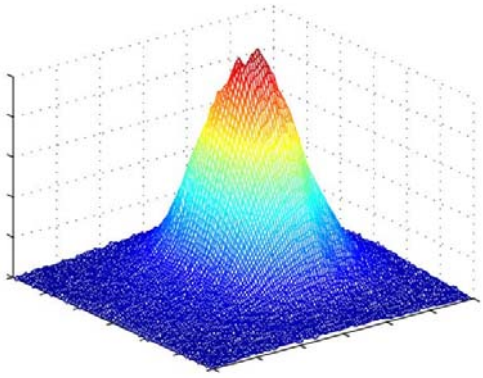

Figure 4.3: Measured idler beam profile

4.3.2 Ring resonator

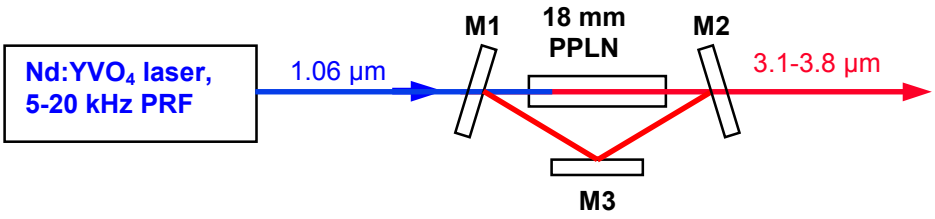

Figure 4.4: Ring OPO configuration

The next series of experiments were performed with the 3-mirror ring OPO configuration shown in Figure 4.4, using the same pump source as in Section 4.3.1. By employing a ring resonator we avoided the use of a Faraday isolator. Also, the ring geometry ensured negligible pump and idler feedback, reducing possible problems with backconversion. The round-trip geometrical length was about 67 mm, which gave approximately the same round-trip time (0.3 ns) as for the linear resonator. Mirror M1 was the same as in Figure 4.1. The output coupler M2 was flat and had reflectivities of approximately 5 %, 76 %, and 9 % for the pump, signal and idler waves, respectively. In the initial experiments M3 was a flat gold-coated mirror. This mirror was damaged during the experiments and was replaced by another gold-coated mirror with 2 m radius of curvature. Unless otherwise stated, the presented results are for the flat M3. The PPLN crystal used in these experiments was 1 mm thick and 18 mm long (originally the crystal was 19 mm long, but it was repolished and recoated after it had been damaged). The pump diameter was approximately 460 µm ($FW1/e^2M$), i.e. approximately the same as in the previous section.

A fairly extensive experimental investigation was carried out with this configuration, including measurements at different pulse rates, measurements for different PPLN grating periods, measurement of idler wavelength as a function of PPLN temperature and pump power, and measurement of idler beam quality. Change of grating period was achieved by translating the entire resonator assembly vertically (normal to the paper plane in Figure 4.4), keeping the pump beam in a fixed vertical position.

Figure 4.5 shows the measured idler pulse energy as a function of pump energy for 3 different pulse rates, 5, 10, and 20 kHz. The PPLN grating period was 29.1 µm and the temperature 190 °C, yielding an idler wavelength of about 3.52 µm. The idler energy values are corrected for a 12 % loss in optical filters, which were used to block the remaining pump and the signal at the OPO output. The pump energy is the total pump energy incident on M1 (which transmits only 85 % of the pump).

There seems to be no significant dependence on pulse rate, indicating that there is little influence from thermal effects, which might arise from a small residual absorption at any of the wavelengths involved. Note that there is a variation in average pump power from 3.75 W

(at 5 kHz) to 15 W (at 20 kHz) at the highest pulse energy. It should be remarked that it was generally necessary to make small adjustments of the resonator alignment in order to maximize the idler energy, as the pump power was raised from threshold and up to the maximum value. This was achieved by a small tilt adjustment of M2. The adjustment was particularly critical close to the pump threshold.

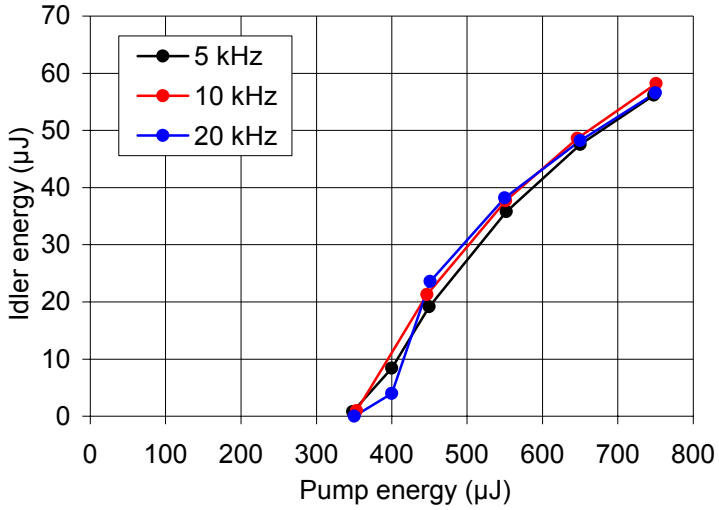

Figure 4.5: Idler pulse energy as a function of pump energy at different pulse rates.

Similar experiments were performed with 3 of the 8 grating periods available on our PPLN crystal, 29.9, 29.1, and 28.5 µm periods, yielding 3.11, 3.52, and 3.77 µm idler wavelength at 190 °C crystal temperature. As in Figure 4.5, we found that there was little dependence on the pump pulse rate. Results obtained with the 3 grating periods are shown in Figure 4.6 for 20 kHz pulse rate. The average idler output power is shown as a function of the pump power. As mentioned above, it became necessary to change mirror M3 (from flat to 2 m radius of curvature) during the experiments, and the data shown in the figure have therefore not all been obtained under exactly the same experimental conditions. However, this seems to have relatively little influence, at least at the highest pump powers, where the curves at 3.52 µm wavelength converge to approximately the same value for both mirrors. There are some inconsistencies near threshold (i.e. the lower threshold at 3.52 µm than at 3.11 µm with the curved M3), but this may have been due to small differences in the OPO alignment. At the maximum pump power we observe an increase in the idler output power for decreasing idler wavelength. This dependence is expected, due to the increasing idler photon energy and assuming an approximately constant number of idler photons per pulse.

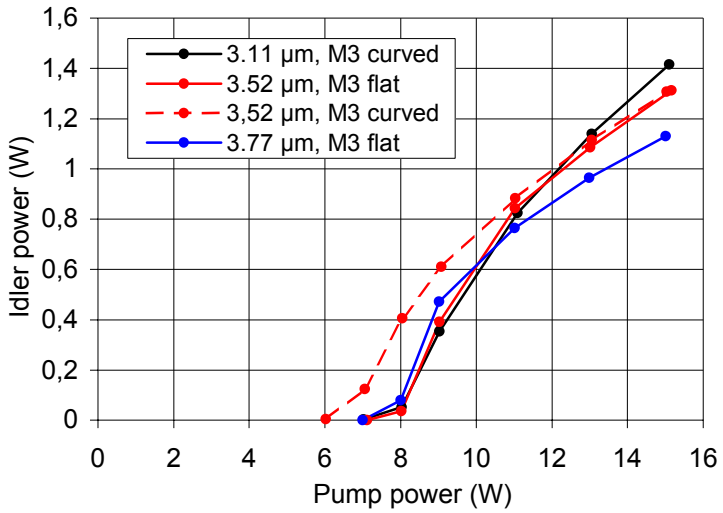

Figure 4.6: Measured idler power as a function of pump power. The measurements were made at 20 kHz pulse rate. The curved M3 had a 2 m radius of curvature.

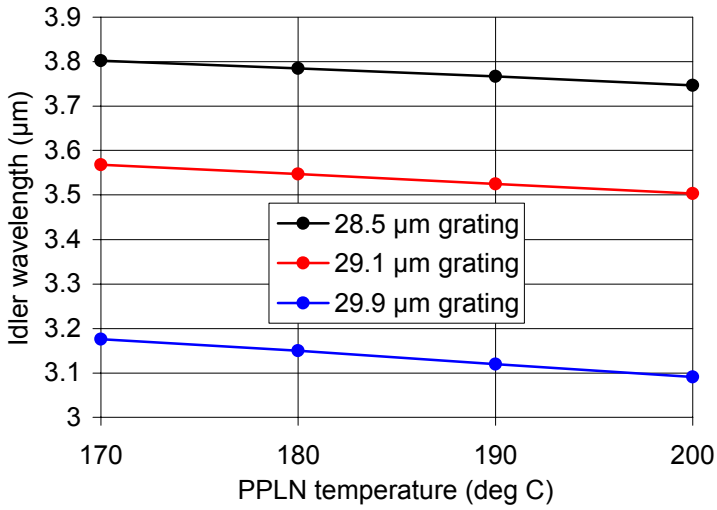

Figure 4.7: Temperature dependences of idler wavelength for 3 different PPLN gratings. The data were taken at 20 kHz pump pulse rate and 15 W average pump power. The wavelengths measured at 10 kHz pulse rate and 5 W average pump power were approximately 4 nm larger for all 3 gratings

In Figure 4.7 we show the measured idler wavelength as a function of the PPLN temperature for the 3 grating periods. The results are in good agreement with phase-matching calculations using the most recent published data for the Sellmeier coefficients of PPLN [21]. It can be added that for all 3 gratings we observed a wavelength shift of approximately 4 nm when the average pump power was changed from 5 W (500 µJ at 10 kHz) to 15 W (750 µJ at 20 kHz). This wavelength shift corresponds to a temperature change of 1.5-2 K in the PPLN crystal, which is most probably due to a small absorption at one or more of the wavelengths involved. A rough estimate indicates that an absorption coefficient on the order of 0.003/cm for the pump and signal could lead to such a temperature increase.

Finally, measurements were performed in order to determine the beam quality of the idler beam under different operating conditions for this OPO configuration. The measurements were made by focusing the idler beam to a waist diameter of a few 100 µm and measuring the beam profile with a pyroelectric camera (Spiricon, model Pyrocam I) at a number of axial positions at both sides of this waist. For every position, a Gaussian beam profile was fitted to the measured profile in both transverse directions (x and y), and the beam diameter (2ω) at each position was defined as the FW1/e^{2}M diameter of the fitted Gaussian profile. The measured fitted beam radius, ω(z), was then plotted as a function of the axial position, z, and the beam quality given by the commonly used parameter, M^2, was then found by fitting the following function to the measured data:

$$\omega(z) = \omega_0 \left[1 + \left(M^2 \frac{z}{z_0} \right)^2 \right]^{\frac{1}{2}} \tag{4.1}$$

where ω_0 is the beam radius at the waist position, z=0, and z_0 is the Rayleigh length defined by:

$$z_0 = \frac{\pi \omega_0^{\,2}}{\lambda} \tag{4.2}$$

where λ is the idler wavelength.

An example of such a fit for the beam radius in the x-direction at 3.11 µm idler wavelength, with 15 W pump power at 20 kHz pulse rate, is shown in Figure 4.8.

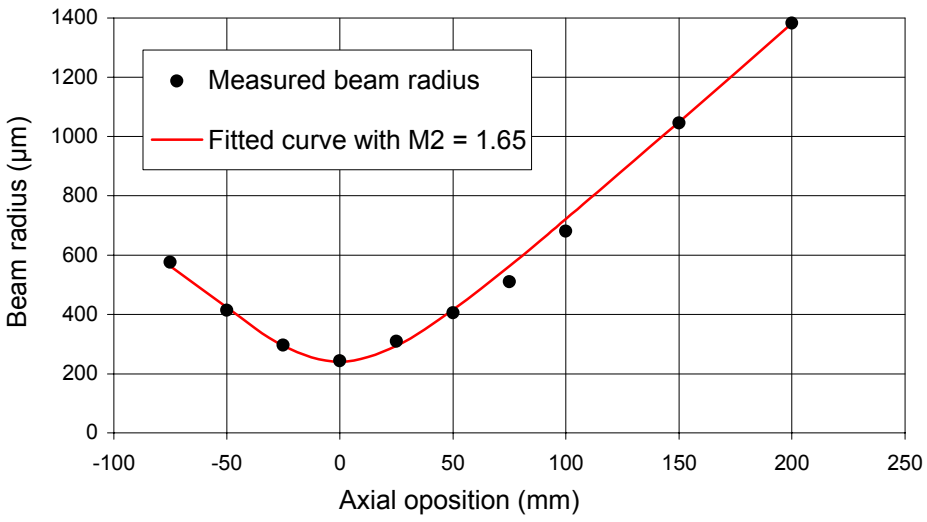

Figure 4.8: Fit of function (4.1) to the measured beam radius in the x-direction for 3.11 µm idler wavelength, 15 W pump power, and 20 kHz pulse rate. The best fit is obtained for a beam quality M^2=1.65, and a beam waist radius ω_0 =240 µm.

Wavelength (µm)	Pump power (W)	Pulse rate (kHz)	M_x^2	M_y^2
3.11	15	20	1.65	1.66
3.52	14 9 3.5 2.25	20 20 5 5	1.27 1.57 1.43 1.66	1.32 1.60 1.72 1.77
3.77	14	20	1.41	1.49

Table 4.1: Measured beam quality. The uncertainty in the measured values is approximately +/-0.1.

A summary of the M^2 values measured under different conditions is given in Table 4.1. It is not clear, however, how the results should be interpreted. The beam quality is fairly good under all conditions, and some of the variations may have been caused by variations in the OPO alignment. The M^2 values are in the range of about 1.3-1.7, i.e. somewhat poorer than the beam quality of the pump (≈1.2). The data for 3.52 µm wavelength seem to indicate that there is an improvement in the beam quality for increasing average pump power, at least for a given pulse rate. In general, the beam quality will be affected by the overlap of the pump beam and the resonator mode of the signal. This, in turn, will be determined by the mirror distances and curvatures, by thermal lens effects (increasing with increasing pump power), and by gain guiding effects (increasing with increasing pump pulse energy). In addition, back-conversion may lead to reduced beam quality at high pump pulse energies. The measurement at 3.11 µm is the only one taken with the curved M3 mirror, and this seems to have resulted in a slightly poorer beam quality.

4.3.3 Monolithic linear resonator

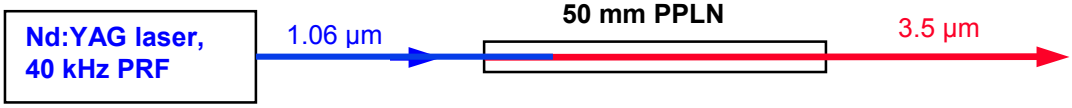

Figure 4.9: Monolithic PPLN OPO

The next configuration studied in pulsed mode of operation is shown in Figure 4.9. In this case we used a Nd:YAG laser developed at FFI, which gave very short pulses at high pulse rate. The pulse rate increased from 6.5 ns at 10 kHz to 10.5 ns at 40 kHz. With such short pulses, a long PPLN crystal, and a small pump spot, we hoped to achieve sufficient parametric gain to obtain efficient conversion to the signal and idler by optical parametric generation (OPG) in a single pass through the crystal, i.e. without optical feedback, as demonstrated previously in [22]. The experiment was set up as in Figure 4.9, with a 50 mm long by 1 mm thick AR-coated PPLN crystal, without any OPO mirrors. However, we soon realized that the optical feedback from the AR-coated crystal ends (about 1 % for both signal and idler) was sufficient to turn the

device into a parametric oscillator, resulting in considerably lower pump thresholds than expected for an OPG.

Experiments were performed at pulse rates from 10 kHz to 65 kHz, and with 2 different focused pump spot radii at the center of the PPLN crystal: 50 μm and 85 μm ($HW1/e^2M$). The beam quality of the Nd-laser was approximately $M^2 = 2$, which resulted in calculated Rayleigh lengths inside the PPLN for the 2 pump spot sizes of approximately 8 mm and 23.5 mm. The maximum pump pulse energy used in the experiments was approximately 200 μJ, and from the pump beam data given above, we calculate the following peak fluences, assuming Gaussian beam profiles:
For 50 μm pump radius: 5 J/cm^2 at the center of the crystal and 0.5 J/cm^2 at the ends
For 85 μm pump radius: 1.8 J/cm^2 at the center of the crystal and 0.8 J/cm^2 at the ends

In reality the beam profiles differed significantly from a Gaussian, particularly at the crystal ends, where the peak fluence was about a factor of 2 higher than calculated. The fluences at the crystal ends were therefore in a range (1-1.5 J/cm^2) where one might expect problems with surface optical damage. The bulk damage threshold for PPLN is uncertain, but as we shall see below we experienced one incident of bulk damage at the center of the crystal.

Results obtained at 10, 20, and 40 kHz pulse rate are shown in Figure 4.10. At 40 kHz pulse rate the measurements were made with both pump spot sizes (50 μm and 85 μm spot radius), and for the largest spot size the measurement was also repeated with a standard OPO input mirror at the input side of the PPLN in order to enhance signal feedback and reduce the OPO threshold. The mirror was HR-coated for the 1.5 μm signal and had about 5 % reflectance for the pump and the 3.5 μm idler. The results obtained for 50 μm pump spot radius indicate that the threshold pump energy decreases slightly for decreasing pulse rate (upper graph). The reason for this is most likely that the pulses are shorter, with higher peak intensity, at low pulse rates. However, for high pump energy the idler energy increases with increasing pulse rate, which could be due to stronger back-conversion at low pulse rate. At 40 kHz pulse rate the pump threshold is less than 1.5 W and the idler power is almost 1 W at 5.3 W pump. The conversion efficiency is more than 18 %, which is more than a factor of 2 higher than with the other OPO configurations discussed above. The reason for the higher efficiency in this case could be reduced back-conversion due to the low signal and idler feedback.

At 40 kHz pulse rate a bulk damage occurred in the center of the crystal when the pump power passed 6 W and the idler power passed approximately 1.2 W. It is not clear what caused the damage, because the pump pulse energy was lower at this point than at the maximum pulse energy points at 10 kHz and 20 kHz pulse rates. Those measurements had been made a short time in advance at the same location in the PPLN crystal, and no damage problems were observed. It could be that the high average intensity (about 150 kW/cm^2) in combination with the high fluence per pulse caused the damage.

The incident with bulk damage led us to increase the pump beam spot radius from 50 μm to 85 μm. As shown in Figure 4.10, this led to a significant increase in the pump threshold as well as a reduction of the slope efficiency. As a result, the idler power obtained at 8 W pump was smaller than the power obtained at 5.3 W pump with 50 μm pump spot radius. The use of an

external mirror at the pump input side, as discussed above, resulted in a decrease of the pump threshold, but the idler power was still lower than that obtained with the small pump spot. Experiments were also carried out at 65 kHz pulse rate, with 85 µm pump spot radius, and up to 14 W pump power, but the idler output was still only about 0.8 W without the external mirror and about 1.1 W with that mirror.

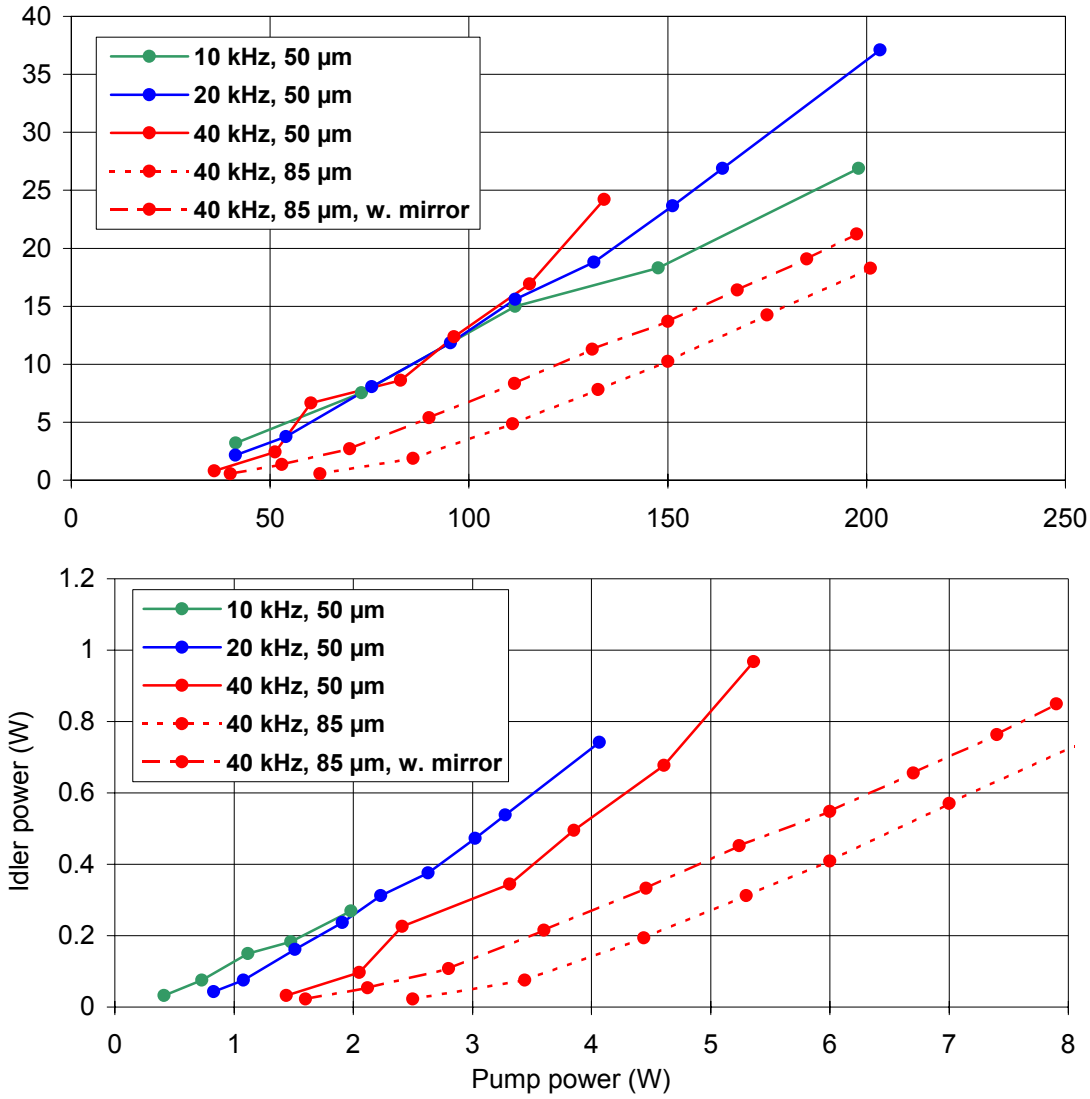

Figure 4.10: Measured 3.5 µm idler pulse energy (upper graph) and power (lower graph) with the monolithic PPLN OPO. The curve marked "w. mirror" indicates that a mirror which is highly reflective for the 1.5 µm signal, is placed at the pump input side of the PPLN. The mirror had an AR coating for the pump and about 5 % reflectance for the idler.

In order to maximize the efficiency it is clearly preferable to use the smallest pump spot size and a pulse rate in the 20-40 kHz range. However, problems with bulk optical damage prevents pumping with more than approximately 5-5.5 W. Since our available pump power is about 18 W, it would be possible to pump 3 separate monolithic OPOs and obtain a total idler power of about 3 W in this configuration.

4.3.4 Linear OPO with long-pulse- and low-beam-quality pumping

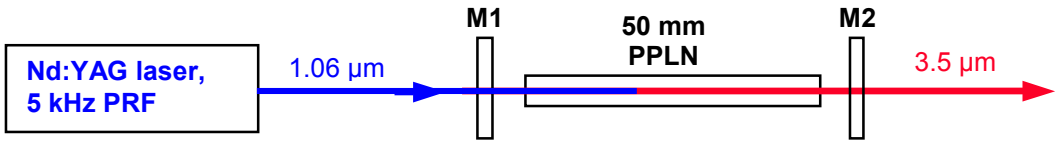

Figure 4.11: Linear OPO configuration with 50 mm long PPLN. The distance between M1 and M2 was 70 mm.

The final configuration studied in pulsed mode of operation is shown in Figure 4.11. The pump source in this case was a Nd:YAG laser with long pulse length and poor beam quality, and we wished to investigate how this would affect the OPO performance. The Nd:YAG pulse rate was 5 kHz, and the maximum average pump power was about 13 W. The pump pulse switched randomly between the two temporal shapes shown in Figure 4.12, indicating switching between two different spatial mode distributions. The FWHM pulse lengths are about 200 ns and 300 ns, respectively. The beam quality, measured in terms of the M^2 value, was about 9.5 in the horizontal direction and 7.5 in the vertical direction.

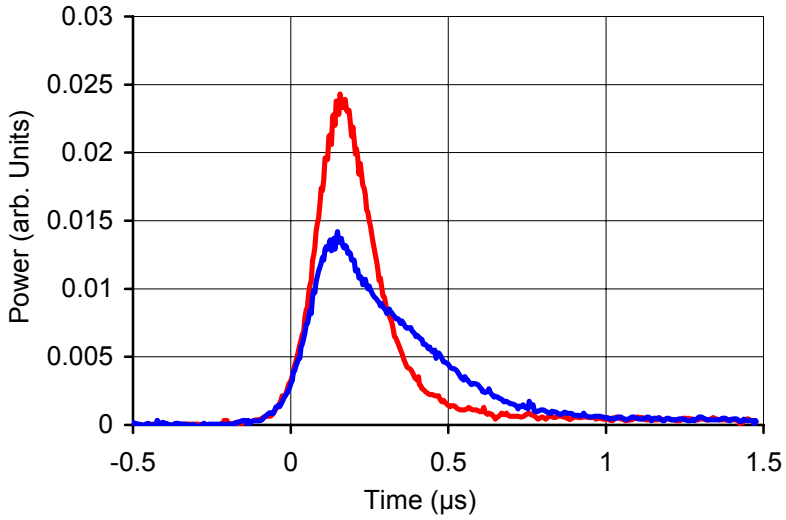

Figure 4.12: Pump pulse shapes. The pump pulse switched randomly between the two shapes.

The pump source was first tested with the ring OPO configuration shown previously in Figure 4.4, but the OPO gain was not sufficient to reach threshold for pump fluences up to 2 J/cm^2. We therefore decided to use a 50 mm long PPLN crystal, as shown in Figure 4.11. The OPO mirrors M1 and M2 are the same as in Figure 4.4, i.e. with 25 % output coupling in M2. The pump beam was focused to a waist diameter of about 0.5 mm (FW1/e^{2}M) at the center of the PPLN crystal, resulting in a fluence of about 2 J/cm^2 at the highest pump power of 12.5 W. Using a crystal grating period of 28.9 µm and 190 °C crystal temperature, the idler wavelength became about 3.6 µm. Under these conditions, we obtained the results shown in Figure 4.13.

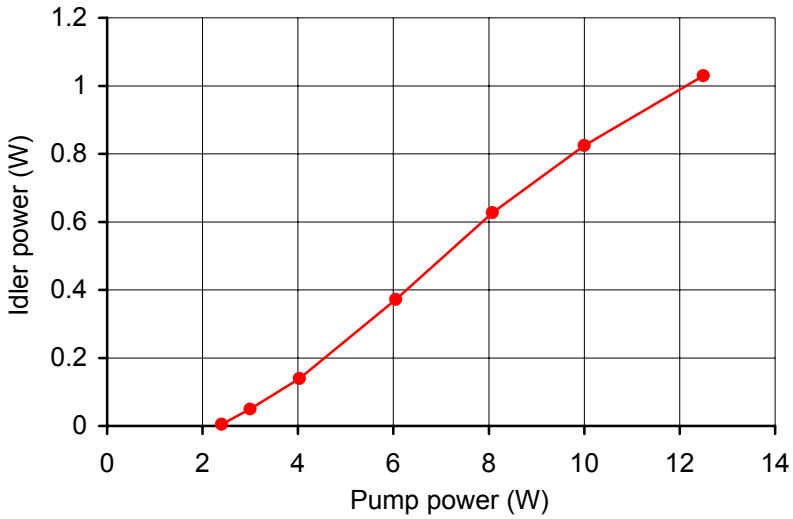

Figure 4.13: 3.6 µm idler output power as a function of the pump power. The idler power is corrected for a 6 % loss in a filter, which was used to block the residual pump and the signal at the output.

The pump threshold is about 2.3 W, and more than 1 W of 3.6 µm idler output power is obtained at 12.5 W pump, corresponding to a conversion efficiency of about 8 %. This is approximately the same conversion efficiency as that obtained in Sections 4.3.1 and 4.3.2, showing that the PPLN OPO is quite tolerant to poor-beam-quality pump beams, and that the lower gain caused by long pump pulses may be compensated by using longer crystals. The measured beam quality of the idler beam was in fact slightly better than that of the pump, with M^2 values of 8.5 and 5.7 in the horizontal and vertical directions, respectively.

Shown below are also the measured pulse shapes of the input pump, transmitted pump, and the idler at 9 W pump power.

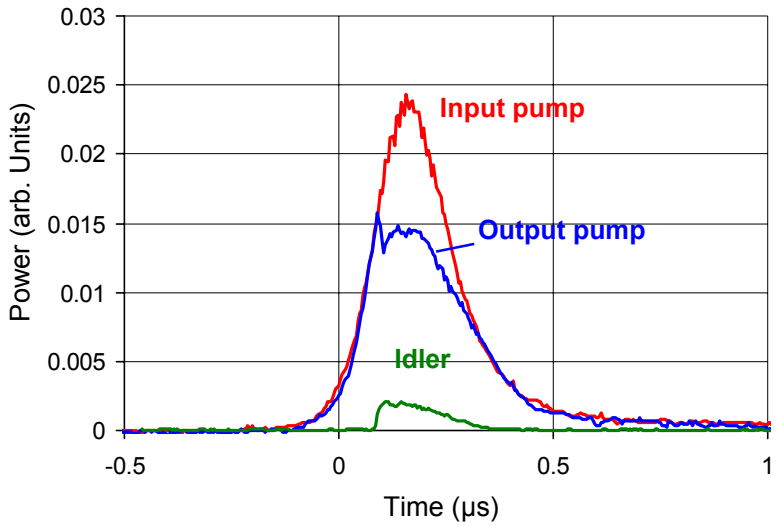

Figure 4.14: Measured pulse shapes at 9 W pump power.

4.4 Continuous-wave operation

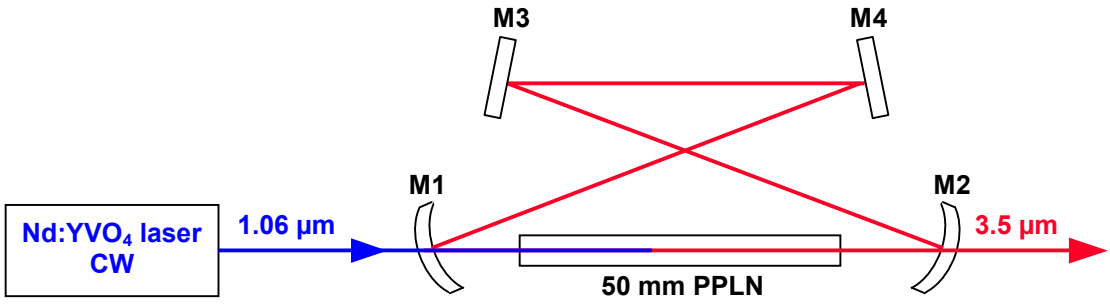

Figure 4.15: Ring OPO configuration for cw operation.

Experiments with cw operation were performed with the ring resonator configuration shown in Figure 4.15. The configuration is similar to the configuration described in references [17] and [20], which reported an idler output power of 3.5 W at 3.25 µm with 13.5 W pump power. The conversion efficiency in those experiments was as high as 80 % of the quantum limit and shows that cw operation holds promise for providing more efficient conversion than pulsed operation. This achievement relies on the fact that cw OPOs are not limited by signal build-up time, and that the cw pump can be focused to a very small spot size without risking optical damage. In addition, the PPLN crystal must be relatively long (typically 50 mm), and all the OPO mirrors must be highly reflective for the signal in order to reduce the roundtrip resonator loss to a minimum and ensure sufficient gain to operate well above threshold. The main disadvantage of this configuration is that most of the 1.5 µm signal will be lost inside the resonator and will therefore not be available as useful output from the OPO. However, if the 3-4 µm idler is the main wavelength of interest, this may not be a problem.

The pump laser in Figure 4.15 is the same as the one described in Section 4.3.1, but with the Q-switch disabled to achieve cw operation. The pump was focused to a spot radius of about 65 µm ($HW1/e^2M$) at the center of the 50 mm long PPLN crystal. The OPO input and output mirrors (M1 and M2) had 100 mm radius of curvature and were separated by 154 mm (geometric distance). The two other mirrors were flat and positioned such that the total geometric resonator round-trip distance was about 464 mm. The waist radius of the resonator mode at the signal wavelength, at the center of the PPLN crystal, was about 75 µm under these conditions, i.e. slightly larger than the pump spot radius. All 4 mirrors had the same coating and had reflectances of about 7 %, 100 %, and 5 % for the pump, signal, and idler, respectively. The low reflectance for the idler at all 4 mirrors ensured perfect singly resonant operation. The PPLN crystal was the same as in Section 4.3.3, and had reflections losses at each end of about 3 %, 1 %, and 1 % for the pump, signal and idler, respectively. We believe that the total round-trip signal loss in the coatings was less than 3 %. The PPLN temperature was kept at 180-190 °C, and the idler wavelength was about 3.5 µm (29.1 µm grating period).

The alignment of the OPO was not trivial. We first tried to use a He-Ne alignment beam, but found that the intensity became too weak after one round-trip. It is also a problem that the OPO gain is very small, so the alignment becomes very critical. Eventually, we found that the

best method was to operate the pump laser in Q-switched mode during the initial alignment of the resonator and use the small amount of frequency-doubled pump (green light) as the alignment beam. The advantage of using the frequency-doubled pump is that it is automatically aligned with the pump. It is important, however, to use a low average pump power during this operation in order to avoid optical damage, especially because of the high finesse of the OPO resonator at the signal wavelength in this case. The fine adjustment of the alignment should therefore be done after the pump is switched back to cw mode.

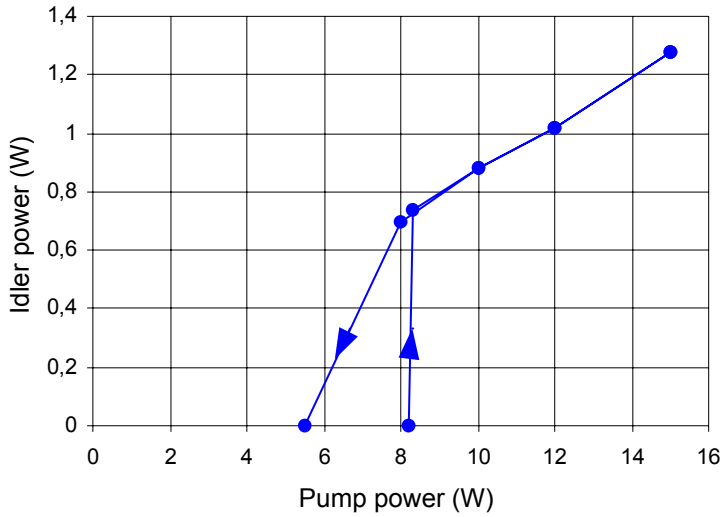

Figure 4.16: 3.5 µm idler output power for the cw PPLN ring OPO.

The measured idler output power as a function of the pump power is shown in Figure 4.16. As indicated, there is a hysteresis in the input-output curve near the pump threshold. We generally found that the output power would increase quite abruptly at a fairly high pump threshold (about 8 W in the case shown here) and then increase slowly as the pump power was raised to the maximum value of about 15 W. The maximum idler power is about 1.3 W in the case shown, which corresponds to a conversion efficiency of about 8.5 %. As the pump power was lowered, the OPO would oscillate down to a significantly lower threshold value. The reason for this behavior has not been clarified, but we suspect that thermal lens effects in the PPLN may play an important role. In fact, the alignment of this OPO turned out to be very critical, and there were significant (up to 20 %) slow fluctuations in output power even after the alignment had been optimized. These fluctuations may be caused by a complicated interplay between the thermal lens caused by the pump, signal, or idler, as well as thermal wedge effects caused by an asymmetry in the transverse heat conduction away from the pumped region.

The absorption coefficient of our PPLN crystals in the transparent wavelength region is specified by the manufacturer to be < 0.15 %/cm. Measurement of crystal heating did however indicate an absorption coefficient of about 0.25 %/cm at the pump wavelength. In a cw OPO the main source of heating could be absorption of the signal. Due to the low signal output coupling, the circulating intracavity signal power will be in the range of 100 W in our experiment, and the absorbed signal power could be in excess of 1 W. This will lead to a quite severe thermal lens and mode distortions, which would limit the achievable efficiency in our experiment. It is possible that the crystals used by other research groups in cw PPLN OPO

experiments did have lower signal absorption, and that this can explain the higher efficiencies obtained by those groups [20, 23]. Another possible important factor could be the susceptibility of the crystals to photorefractive effects, which may depend on the crystal fabrication technique.

A plot of the idler output beam profile is shown in Figure 4.17. The beam profile is severely distorted, which could be caused by the thermal effects discussed above. However, further experiments with crystals from different manufacturers will be required in order to make firm conclusions about the cause and solutions to these problems.

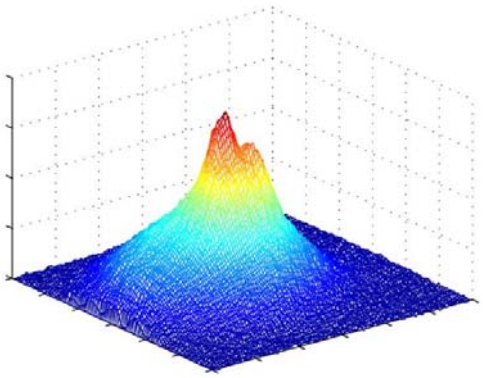

Figure 4.17: Idler beam profile of the cw PPLN OPO

5 CONCLUSIONS

A study has been conducted of mid-infrared OPOs based on PPLN as the nonlinear optical material. Experiments have been performed with a number of 1.06 µm pump sources (Nd:YAG and Nd:YVO_4) and OPO resonator configurations, in both pulsed and cw mode of operation. Good performance has been obtained with idler wavelengths covering the 3.1-3.8 µm region, which was accessible by using the different periodic poling gratings available in our PPLN crystals. In nearly all cases, the measured pump-to-idler conversion efficiency was in the range of 7-9 %, and the idler output power was in the range of 1-1.4 W. A notable exception was the experiment described in Section 4.3.3, with the monolithic OPO resonator and short pump pulse (<10 ns). In this case, an efficiency of 18 % and an output power of almost 1 W was obtained at 5.3 W pump power. This was the maximum pump power that could be used without risking optical damage. Using all the available pump power to pump 3 different monolithic OPOs (possibly on the same PPLN crystal), there is potential of achieving 3 W of mid-infrared output at different wavelengths with this configuration. The reason for the higher efficiency in this case could be reduced back-conversion due to the low signal and idler feedback, provided by the imperfect AR-coatings on the PPLN crystal end-faces.

It is also worth noticing, as discussed in Section 4.3.4, that an acceptable conversion efficiency can be obtained, even if the pump has quite poor beam quality (M^2 = 7-9) and long pulses (> 200 ns). The lower gain in this case could be compensated for by increasing the PPLN crystal length. The beam quality of the idler was also slightly better than that of the pump.

The conversion efficiency obtained in cw mode of operation (8-9 %) is more than a factor of 2 below the highest values reported in the literature [20, 23]. A possible explanation could be that our crystals had higher absorption at the pump and signal wavelengths, causing strong heating and thermal lens effects. This problem will have to be studied in more detail by comparing results obtained with PPLN crystals from different manufacturers.

In conclusion, PPLN-based OPOs are convenient sources of mid-IR radiation in the 3-4 μm region. The conversion efficiency, using a 1 μm pump, is typically below 10 %, but it can be increased considerably, as found in the experiments with the monolithic OPO in Section 4.3.3. We have established mid-IR sources with output powers above 1 W, suitable for use in countermeasure-tests against military infrared sensors in the laboratory.

References:

[1] NEMESIS DIRCM system – AN/AAQ-24(V), manufactured by Northrop Grumman and BAE Systems

[2] ATIRCM system – AN/ALQ-212(V), manufactured by Lockheed Sanders (now BAE Systems)

[3] G Rustad, E Lippert and K Stenersen (2001):
"Beam shaping of high power laser diode bars", FFI/RAPPORT – 2001/02647

[4] K Stenersen, E Lippert, G Rustad and G Arisholm (2001):
"Thermal effects in end-pumped solid state lasers – influence on resonator stability, beam quality, and output power", FFI/RAPPORT – 2001/03865

[5] G Arisholm, E Lippert, G Rustad and K Stenersen (2000):
"Effect of resonator length on a doubly resonant optical parametric oscillator pumped by a multi-longitudinal-mode beam", Opt Lett, Vol 25, 1654-7

[6] G Rustad, E Lippert, K Stenersen and G Arisholm (2001):
"Enhanced power from a doubly resonant optical parametric oscillator by choice of resonator length",
OSA Trends in Optics and Photonics on Advanced Solid-State Lasers, Vol 50, 660-5

[7] G Arisholm, G Rustad and K Stenersen (2001):
"Importance of pump-beam group velocity for backconversion in optical parametric oscillators", J Opt Soc Am B, Vol 18, 1882-90

[8] G Arisholm (2002):
"Optical parametric oscillator for narrow-band conversion to a single polarization",
OSA Trends in Optics and Photonics on Advanced Solid-State Lasers, Vol 68

[9] G Arisholm, E Lippert, G Rustad and K Stenersen (2002):
"Efficient conversion from 1 μm to 2 μm by a KTP-based ring parametric oscillator",
Opt Lett (accepted for publication 2002)

[10] G Arisholm, M Haakestad, E Lippert, G Rustad and K Stenersen (2002):
EUCLID RTP 8.7 – ADMIRAL
Workpackage 4: High pulse rate 3-5 μm source, Final report, May 2002

[11] R W Boyd (1992):
"Nonlinear Optics", Academic Press, San Diego

[12] M M Fejer, G A Magel, D H Jundt and R L Byer (1992):
"Quasiphasematched second harmonic generation: Tuning and tolerances",
IEEE J Quantum Electron, Vol 28, 2631-54

[13] E Lallier, M Brevignon and J Lehoux (1998):
"Efficient second-harmonic generation of a CO_2 laser with a quasi-phase-matched GaAs crystal", Opt Lett, Vol 23, 1511-13

[14] L A Eyres, P J Tourreau, T J Pinguet, C B Ebert, J S Harris, M M Fejer, L Becouarn, B Gerard and E Lallier (2001): "All-epitaxial fabrication of thick, orientation-patterned GaAs films for nonlinear optical frequency conversion", Appl Phys Lett, Vol 79, 904-6

[15] M Yamada, N Nada, M Saitoh and K Watanabe (1993): " First-order quasi-phasematched $LiNbO_3$ waveguide periodically poled by applying an external field for efficient blue second-harmonic generation", Appl Phys Lett, Vol 62, 435-6

[16] L E Myers, R C Eckhardt, M M Fejer, R L Byer, W R Bosenberg and J W Pierce (1995): "Quasiphasematched optical parametric oscillators in bulk periodically poled $LiNbO_3$", J Opt Soc Am B, Vol 12, 2102-16

[17] L E Myers and W R Bosenberg (1997): "Periodically poled lithium niobate and quasi-phase-matched optical parametric oscillators", IEEE J Quantum Electron, Vol 33, 1663-72

[18] H Karlsson and F Laurell (1997): "Electric field poling of flux grown $KTiOPO_4$", Appl Phys Lett, Vol 71, 3474-6

[19] G T Kennedy, D T Reid, A Miller, M Ebrahimzadeh, H Karlsson, G Arvidsson and F Laurell (1998): "Near- to mid-infrared picosecond optical parametric oscillator based on periodically poled $RbTiOAsO_4$", Opt Lett, Vol 23, 503-5

[20] W R Bosenberg, A Drobshoff, J I Alexander, L E Myers and R L Byer (1996): "93% pump depletion, 3.5-W continuous-wave, singly resonant optical parametric oscillator", Opt Lett, Vol 21, 1336-8

[21] D H Jundt (1997): “Temperature-dependent Sellmeier equation for the index of refraction, n_e, in congruent lithium niobate”, Opt Lett, Vol 22, 1553-5

[22] M J Missey, V Dominic, P E Powers and K L Schepler (1999): “Periodically poled lithium niobate monolithic nanosecond optical parametric oscillators and generators”, Opt Lett, Vol 24, 1227-9

[23] P Gross, M E Klein, T Walde, K J Boller, M Auerbach, P Wessels and C Fallnich (2002): “Fiber-laser-pumped continuous-wave singly resonant optical parametric oscillator”, Opt Lett, Vol 27, 418-20

DISTRIBUTION LIST

FFIE **Dato:** 25 juni 2002

RAPPORTTYPE (KRYSS AV)	RAPPORT NR.	REFERANSE	RAPPORTENS DATO
X RAPP ☐ NOTAT ☐ RR	2002/02830	FFIE/792/115	25 juni 2002
RAPPORTENS BESKYTTELSESGRAD		ANTALL EKS UTSTEDT	ANTALL SIDER
Unclassified		30	31
RAPPORTENS TITTEL		FORFATTER(E)	
MID-INFRARED OPTICAL PARAMETRIC OSCILLATORS BASED ON PERIODICALLY-POLED LITHIUM NIOBATE		ARISHOLM Gunnar, STENERSEN Knut, RUSTAD Gunnar, LIPPERT Espen, HAAKESTAD Magnus	
FORDELING GODKJENT AV FORSKNINGSSJEF		FORDELING GODKJENT AV AVDELINGSSJEF:	
Stian Løvold		Johnny Bardal	

EKSTERN FORDELING

ANTALL	EKS NR	TIL
1		FO/FST
1		FO/FST, v/Oblt Gaute Dyrdal
1		LTI
1		LTI, v/Oblt Erik Pande-Rolfsen
1		FLO/Land, v/Elektro-optisk kontor
1		FLO/Luft
1		FLO/Luft, v/Senioring Richard Nordås
1		FLO/Sjø
1		FLO/Sjø v/Orlkapt Bjarne Isfeldt
		www.ffi.no

INTERN FORDELING

ANTALL	EKS NR	TIL
14		FFI-Bibl
1		Adm direktør/stabssjef
1		FFIE
1		FFISYS
1		FFIBM
1		FFIN
2		Restopplag til Bibl
		Elektronisk fordeling til:
		Halvor Ajer, E
		Gunnar Arisholm, E
		Egil Bingen, E
		Trond Brudevoll, E
		Harald Hovland, E
		Magnus Willum Haakestad, E
		Espen Lippert, E
		Stian Løvold, E
		Stephane Nicolas, E
		Gunnar Rustad, E
		Espen Stark, E
		Knut Stenersen, E
		Asta Storebø Villanger, E
		FFI-veven

FFI-K1 Retningslinjer for fordeling og forsendelse er gitt i Oraklet, Bind I, Bestemmelser om publikasjoner for Forsvarets forskningsinstitutt, pkt 2 og 5. Benytt ny side om nødvendig.